MJFAS
Malaysian Journal of Fundamental and Applied Sciences

RESEARCH ARTICLE

The Role of Slip Velocity in Fractional MHD Casson Fluid Flow within Porous Cylinder

Wan Faezah Wan Azmi, Ahmad Qushairi Mohamad*, Lim Yeou Jiann, Sharidan Shafie

Department of Mathematical Sciences, Faculty of Science, Universiti Teknologi Malaysia, 81310 UTM Johor Bahru, Johor, Malaysia

Abstract Numerous academics are intrigued by exploring the fractional Casson fluid model due to its enhanced precision compared to the traditional fluid model. However, many researchers have successfully tackled the analytical solution for the fractional fluid model while overlooking the impact of boundary slip. Hence, this study aims to tackle the challenge of describing the Casson fluid behaviour with fractional properties in a cylindrical domain, considering the influence of slip velocity at the boundaries. Furthermore, magnetohydrodynamics (MHD) had been introduced into the analysis and considered a porous medium resembling a blood clot or fatty plaque. The Caputo-Fabrizio fractional derivative is employed to establish the dimensionless governing equation. Subsequently, we solve it analytically using the Laplace transform in conjunction with finite Hankel transform techniques. A thorough examination follows the graphical presentation of the analytical solution in the context of relevant parameters. The findings illustrate those higher values of the Casson parameter, slip velocity parameter, Darcy number, and fractional parameter lead to an augmentation in fluid velocity. Conversely, an escalation in magnetic parameters causes a reduction in fluid velocity. These findings can be utilized to validate the accuracy of numerical results. The findings of this study hold considerable importance in enhancing our understanding of human blood flow, especially in scenarios where a velocity gradient occurs between blood particles and the stretching motion of arteries.

Keywords: Casson Fluid, Caputo-Fabrizio Fractional Derivative, MHD, Slip Velocity Cylinder.

Introduction

Categorized based on their intrinsic characteristics, Newtonian and non-Newtonian fluids differ in their adherence to Newton's Law of viscosity. Non-Newtonian fluids, in contrast to their Newtonian counterparts, lack this attribute. This investigation focuses on studying the distinct behavior of a chosen non-Newtonian substance, the Casson fluid, due to its unique propertiesThe material may exhibit characteristics similar to a solid, impeding flow if the applied shear stress surpasses the yield stress. Conversely, it will deform or flow if the situation is reversed, mirroring the hemodynamic traits of blood circulation in the human microvasculature [1], [2]. Batra and Das [3] are pioneers in their early exploration of depicting blood flow within a cylindrical domain using the Casson fluid model. Furthermore, the conductive attributes of blood give rise to magnetohydrodynamic (MHD) properties when subjected to an external magnetic field generated by devices like televisions, laptops, and cellular phones [4], [5]. In investigating the potential constant magnetic field impact on human blood flow, numerical research revealed a negative correlation between the flow rate and magnetic field strength [6]. As part of their investigation, Elshehawey *et al.*, [7] established a mathematical framework for examining a magnetic field's impact and the body's acceleration on blood flow within a cylindrical structure. This model was crafted using analytical techniques. Tzirtzilakis [8] conducted research on the influence of a magnetic field on blood flow through a rectangular duct, with findings aligning with Sud and Sekhon [6]. Exploring blood flow in inclined arteries with the influence of a magnetic field, Sanyal *et al.*, [9] incorporated the body acceleration effect into their analytical study.

Moreover, a porous medium within the cylinder is an intriguing subject of investigation for researchers, as it finds practical relevance in conditions such as blood flow containing fatty plaque or blood clot

***For correspondence:**
ahmadqushairi@utm.my

Received: 26 Nov. 2023
Accepted: 4 Feb. 2024

pathologies [10]. A porous medium is characterized as dispersed interconnected small voids in a solid structure, which occupy a quantifiable fraction of its overall volume [11]. The Newtonian fluid's analytical solution, depicting blood flow, incorporated considerations for periodic body acceleration within a porous medium with stenosis, was derived [12]. Rathod & Tanveer [13] managed to obtain analytical solutions for a model that deals with magnetohydrodynamic (MHD) blood flow, encompassing two viscous fluids flow within a stationary cylinder embedded in a porous medium. After that, Jamil & Zafarullah [14] proceeded to conduct an in-depth study of a similar problem [13], the study involved the analysis of second-grade fluid flow between two cylinders in motion. Previously cited researchers utilized analytical techniques, explicitly employing the Laplace transform and finite Hankel transform methods, to address the complexities discussed. However, it's noteworthy that none of them took into consideration for cylinder’s wall with the influence of slip velocity.

Taking slip velocity into account unveils significant changes in the fluid's velocity pattern, particularly near the boundary. Slip velocity refers to the finite speed observed when two distinct mediums experience relative motion, illustrated by the movement of particles in a viscous fluid as the boundary stretches [15]. Highlighting the practical relevance of slip velocity, Nubar [16] underscores its importance in various contexts, including the flow of blood within arteries. Inspired by its importance in blood flow, certain researchers have acquired and briefly examined analytical solutions for Casson fluid flow in the Cartesian coordinate system [17]–[19]. Padma *et al*., [20], [21], in their research, delved into an analytical investigation of blood flow velocity concerning slip and no-slip boundary conditions within a cylindrical structure, employing the Jeffrey fluid model. Investigating Casson fluid flow within a cylinder, Ahmed & Hazarika [22] and Jalil & Iqbal [23] numerically assessed the influence of slip velocity. However, none of these studies incorporated the fractional fluid model to represent the fluid flow issue.

Fractional calculus has garnered considerable interest in fluid mechanics thanks to its capacity to provide a more exact and true-to-life method in contrast to the traditional calculus approach. Consequently, this surge in interest has created mathematical models that embrace fractional calculus, thereby enhancing the ability to portray fluid behaviour with greater precision [24]. Noteworthy fractional calculus models include the Caputo, Riemann-Liouville, and Caputo-Fabrizio models. The exploration within fractional calculus aims to determine whether fractional, complex, or irrational values align with the n-notation for differentiation or integration [25]. Observations of its applications are evident in the study of fluid mechanics [26], mechanical and electrical properties [27], as well as research in medical and health science [28]. Ali *et al*., [29] performed a thorough analytical analysis to explore how fractional parameters affect the behaviour of the Caputo Casson fluid model within a stationary cylinder exposed to a magnetic field. This research was motivated by the extensive practical applications of such scenarios. The Laplace and Hankel transform methods were deployed to acquire the result. Then, Sene [30] analyzed the fractional operator, analogous to what was presented by Ali *et al.,* [29] in the context of Casson fluid flow over a moving plate. The problems are being addressed via the Laplace transform and Fourier transform to explore how the fractional parameter affects fluid velocity over time.

The method of fractional-order derivatives by Caputo and Fabrizio has been utilized extensively by researchers to address fluid models due to its broad applicability across fields ranging from quantum physics to fluid dynamics. Its ability to surpass the constraints of representing physical phenomena and overcome the challenges associated with a power-law kernel, like the Caputo fractional derivative, underscores the effectiveness of a non-singular kernel [31]. Driven by it, Ali *et al*., [32] examined the impact of MHD in a stationary cylinder while studying human blood flow, which yielded analytical results. Subsequently, they expanded this investigation to include a study involving a moving and oscillating cylinder [33], [34]. An investigation into unsteady blood flow through a stationary cylinder, considering the MHD effect and porosity, was carried out by Maiti *et al*., [35], [36], [37], [38]. Following this, Jamil *et al*., [39]–[41] addressed a similar problem to that explored by [32] but within an inclined cylinder. In all of these studies, the modelling method used was the Caputo-Fabrizio fractional derivative. Analytical solutions are being achieved in numerous studies by integrating the Laplace transform and the finite Hankel transform. Notably, none of these researchers took into account the influence of boundary slip velocity.

Based on the available literature, no previous analytical solution has been found for the Casson fluid’s fractional flow characteristics within a cylindrical configuration of a porous medium. This investigation, unlike previous ones, considers the influence of boundary slip velocity and an external magnetic field’s application. Hence, the examination delves into the behavior of the Casson fluid model within a cylindrical domain is affected by the combined influence of magnetohydrodynamics (MHD), porosity, fractional order, and slip velocity. To achieve this aim, the study formulates the governing equation for momentum analysis using the Caputo-Fabrizio fractional derivative methodology. This investigation, addressing a usual limitation encountered in representing physical phenomena, is achieved by utilizing a non-singular kernel, as opposed to a power-law kernel, in the adopted methodology. The analytical solution for fluid velocity is acquired using the application of Laplace Transform and finite Hankel transform techniques. Afterwards, the analytical findings are visually represented and assessed, considering relevant parameters, using Maple software.

Methodology

Exploring the dynamic flow characteristics of an incompressible Casson fluid, this study investigates its passage through a vertically oriented cylinder of infinite height, with R_0 representing the radius. Within this context, the upward direction along the cylinder aligns with the vertical z-axis, and the R-axis stands perpendicular to the z-axis. The study delves into the dynamic aspects of fluid motion, specifically considering a magnetic field's interplay and a porous medium's presence. The fluid motion's dynamics are affected by both the porous medium and the magnetic field applied from an external source. At the initial time, denoted as $t^*=0$, both of fluid and cylinder are stationary. Subsequently, as $t^*>0$, the fluid sets into motion, and a velocity gradient arises at the cylinder's wall, represented as the slip velocity ξ_s. The variables t and R are the sole factors governing the fluid's velocity. The arrangement of fluid flow is visually depicted in Figure 1.

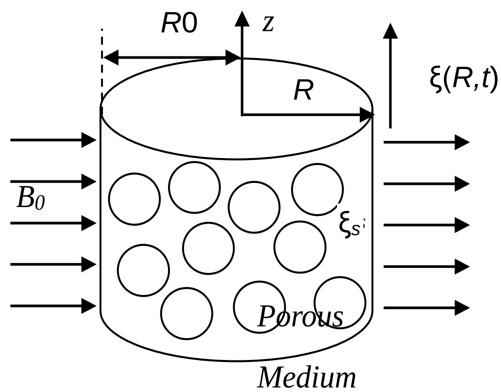

Figure 1. Visual representation of the problem

The provided equation signifies the principal momentum equation [35]

$$\rho\frac{\partial \xi^*\left(R^*,t^*\right)}{\partial t^*}=\mu\left(1+\frac{1}{\chi}\right)\left(\frac{\partial^2\xi^*\left(R^*,t^*\right)}{\partial R^{*2}}+\frac{1}{R^*}\frac{\partial\xi^*\left(R^*,t^*\right)}{\partial R^*}\right)-\frac{\mu}{k_p}\xi^*\left(R^*,t^*\right) -\sigma B_0^2\xi^*\left(R^*,t^*\right), \tag{1}$$

accompanied by initial and boundary conditions [21]

$$\begin{aligned} &\xi^*(R^*,0) = 0 \quad ;\ R^*\in[0,R_0],\\ &\xi^*(R_0,t^*) = \xi_s^* \quad ;\ t^*>0. \end{aligned} \tag{2}$$

Dimensionless variables are introduced as follows: [21], [33]

$$t=\frac{t^*\nu}{R_0^2},\ \ R=\frac{R^*}{R_0},\ \ \xi=\frac{\xi^*}{\xi_0},\ \ \xi_s=\frac{\xi_s^*}{\xi_0}. \tag{3}$$

where fluid density is denoted as ρ, the representation of the velocity component along the z-axis is ξ^*, the fluid dynamic viscosity is indicated as μ, the parameter of the Casson fluid is denoted as χ, permeability constant k_p, electrical conductivity σ, field strength applied magnetic indicated as B_0, average velocity for fluid represented as ξ_0, and kinematic viscosity for fluid denoted as ν. The dimensionless momentum equation can be derived, and its associated initial and boundary conditions can be acquired by replacing equation (3) with equations (1) and (2), which yield as

$$\frac{\partial \xi(R,t)}{\partial t} = \left(1+\frac{1}{\chi}\right)\left(\frac{\partial^2 \xi(R,t)}{\partial R^2} + \frac{1}{r}\frac{\partial \xi(R,t)}{\partial R}\right) - \frac{1}{Da}\xi(R,t) - M\xi(R,t), \qquad (4)$$

and

$$\begin{aligned} &\xi(R,0)=0 \quad ;\ R\in[0,1]\,, \\ &\xi(1,t)=\xi_s \quad ;\ t>0, \end{aligned} \qquad (5)$$

where the obtained dimensionless parameter are $Da=k_p/r_0^2$, Darcy number and $M=\sigma B_0^2 r_0^2/\rho v$, magnetic parameter. Utilizing the model derived from the Caputo-Fabrizio fractional derivative [33] in equation (4) results in

$${}^{CF}D_t^{\alpha}\xi(R,t) = \chi_a\left(\frac{\partial^2 \xi(R,t)}{\partial R^2} + \frac{1}{R}\frac{\partial \xi(R,t)}{\partial R}\right) - \frac{1}{Da}\xi(R,t) - M\xi(R,t), \qquad (6)$$

representing the definition of the Caputo-Fabrizio fractional derivative [35] for $0<\alpha<1$, ${}^{CF}D_t^{\alpha}\xi(R,t) = \frac{1}{1-\alpha}\int_0^{\tau}\exp\left(\frac{-\alpha(\tau-t)}{1-\alpha}\right)\xi'(\tau)\,dt$, and $\chi_a = \chi/(\chi+1)$ is the constant parameter. To equations (5) and (6), the Laplace transform is applied, yielding

$$\frac{a_0 q\bar{\xi}(R,q)}{q+a_1} = \chi_a\left[\frac{\partial^2 \bar{\xi}(R,q)}{\partial R^2} + \frac{1}{R}\frac{\partial \bar{\xi}(R,q)}{\partial R}\right] - \frac{1}{Da}\bar{\xi}(R,q) - M\bar{\xi}(R,q), \qquad (7)$$

and

$$\bar{\xi}(1,q) = \frac{\xi_s}{q}, \qquad (8)$$

where the parameters $a_0 = 1/1-\alpha$, and $a_1 = a_0\alpha$, for fractional constant, $\bar{\xi}(R,q)$ is the Laplace transform of the function $\xi(R,t)$, with q as the transform variable. Subsequently, equation (7) is subjected to the finite Hankel transform with consideration of boundary condition (8), resulting in the following outcome:

$$\bar{\xi}_H(\lambda_n,q) = \frac{\chi_a\lambda_n J_1(\lambda_n)\xi_s}{q}\left[\frac{q+a_1}{q+\dfrac{a_1\left(L+\chi_a\lambda_n^2\right)}{a_0+L+\chi_a\lambda_n^2}}\right]\frac{1}{\left(a_0+L+\chi_a\lambda_n^2\right)}, \qquad (9)$$

where the finite Hankel transform of the function λ_n, denoted as $\bar{\xi}_H(\lambda_n,q) = \int_0^1 R\bar{\xi}(R,q)J_0(R\lambda_n)\,dR$ is expressed with n=0,1,… as the positive roots of the Bessel function equation. Here J_0 and J_1 refer to the Bessel function of the first kind and zero-order/first-order, and $L = M+1/Da$ refer to constant parameter. Simplified equation (9) is as follows

$$\bar{\xi}_H(\lambda_n,q) = \frac{J_1(\lambda_n)}{\lambda_n}\frac{\xi_s}{(1+E[n])}\left[\frac{1}{q} - \frac{a_0}{C[n](q+I[n])}\right], \qquad (10)$$

where $E[n] = 1+(L/\chi_a\lambda_n)$, $C[n] = a_0+L+\chi_a\lambda_n$, $I[n] = a_1\left(L+\chi_a\lambda_n^2\right)/C[n]$, are the constant parameters. Equation (10) undergoes the inverse Laplace transform in the next step, resulting in the expresión as

$$\xi_H\left(\lambda_n,t\right)=\frac{J_1\left(\lambda_n\right)}{\lambda_n}\frac{\xi_s}{E\left[n\right]}\left[1-\frac{a_0\exp\left(-I\left[n\right]t\right)}{C\left[n\right]}\right]. \quad (11)$$

Ultimately,apply the inverse finite Hankel transform to equation (11), leading to the derivation of the velocity profile as given by equation (12).

$$\xi\left(R,t\right)=\xi_s-2\xi_s a_0\sum_{n=1}^{\infty}\frac{J_0\left(R\lambda_n\right)}{\lambda_n J_1(\lambda_n)}\left[\frac{\exp\left(-I\left[n\right]t\right)}{C\left[n\right]}\left(1-\frac{L}{\chi_a\lambda_n^2+L}\right)\right]-2\xi_s\sum_{n=1}^{\infty}\frac{J_0\left(R\lambda_n\right)}{\lambda_n J_1(\lambda_n)}\left[\frac{L}{\chi_a\lambda_n^2+L}\right]. \quad (12)$$

Results and Discussion

To evaluate the credibility of the result, we examine equation (12) in its limit and contrast it with a previously reported outcome by Khan *et al*., [42], as depicted in Figure 2. The graphical evaluation reveals a robust concordance between the two datasets, affirming the precision of the equation (12).

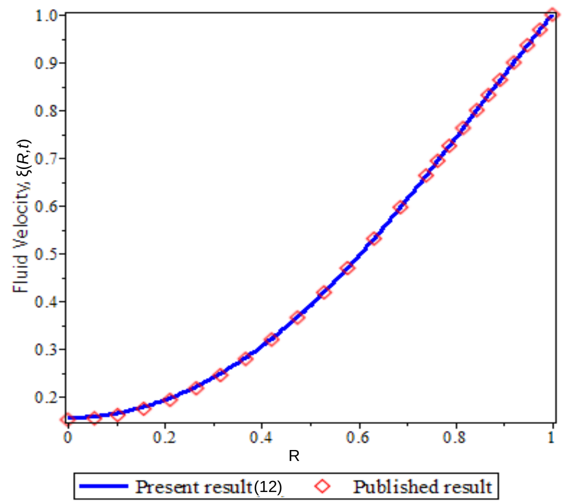

Figure 2. Result Comparison: Current Study (χ =Da=∞, ξ_s=1, M=0, α=0.999) vs. Published Data (Gr=ω=0)

The analytical solutions are presented for fluid velocity as outlined in equation (12) to gain a deeper comprehension of Casson fluid flow behaviour. Key parameters, such as the including the Casson parameter χ, magnetic parameter M, Darcy number Da, slip velocity parameter ξ_s, fractional parameter α, and time parameter t are considered in the analysis. Figures 3 to 10 illustrate how these parameters influence the behaviour of Casson fluid.

The illustration in Figure 3 reveals the impact of the Casson parameter on fluid velocity. Increasing the Casson parameter results in the velocity profile expansion. Notably, at R=0.5, there is a 36.30% increase in fluid velocity when transitioning from χ=0.4 to χ=2.0. This heightened fluid velocity can be attributed to a decrease in fluid yield stress resulting from the elevated Casson parameter, leading to a thinner boundary layer and an increase in flow velocity.

Figure 4 illustrates how the velocity profile is affected by changes in the magnetic parameter. According to the results, increased values of the magnetic parameter are associated with a reduction in fluid velocity. For instance, when considering R=0.5, there is a 32.40% decrease in fluid velocity as we transition from M=0 to M=2. Upon the external magnetic field application, a conductive fluid undergoes induction of an electric current, leading to the emergence of the Lorentz force. This force, a consequence of the interaction between magnetic fields and the induced currents, acts as a resistive force that impedes the fluid's motion, giving rise to the observed phenomenon.

Figure 5 portrays the impact of porosity, as represented by Darcy's number, on fluid velocity. The trend reveals that increasing the Darcy number leads to higher velocity profiles. For instance, at R=0.5, there is a 12.69% increase in fluid velocity when transitioning from Da=1 to Da=3. Due to this phenomenon, the incremento f the the Darcy number is attributed to a rise in the permeability of the porous médium. Consequently, the porous medium becomes more capable of transmitting fluid particles, thereby enhancing fluid velocity.

Furthermore, Figures 6 and 7 depict how the fluid velocity is affected by changes in the fractional parameter. It shows that if the fractional parameter increases within the range of 0<α<1, coupled with a slip velocity effect, it results in higher fluid velocity over an extended period (t=1.0). On the other hand, higher fluid velocity is achieved by decreasing the fractional parameter within a shorter time interval (t=0.1). This difference can be explained by the memory effect of the fractional derivative, which introduces variations between small and large time intervals. Notably, there is a 71.27% increase in fluid velocity for α=1, while a 17% increase is observed for α=0.5. Utilizing the fractional Casson fluid model, one achieves a finer depiction of fluid velocity, especially when the α value is configured as 1, in contrast to the classical Casson fluid model.

Furthermore, in Figures 3-6, we can analyze the repercussions of slip velocity at the boundary (r=1). Observational data suggests that when the slip velocity phenomenon intensifies, there is a simultaneous augmentation in fluid velocity at the cylinder's surface. For instance, R=0.5, there is a 50% increase in fluid velocity when transitioning from ξ_s=0.2 to ξ_s=0.4. This occurrence can be ascribed to the notable speed differentiation that arises at the boundary where fluid particles meet the cylinder's boundary. Moreover, fluid velocity increases as time progresses towards the center's cylinder (R=0). Since the slip velocity effect is a real-world occurrence, notably in scenarios like blood circulation within arterial vessels, its incorporation into this study is deemed relevant.

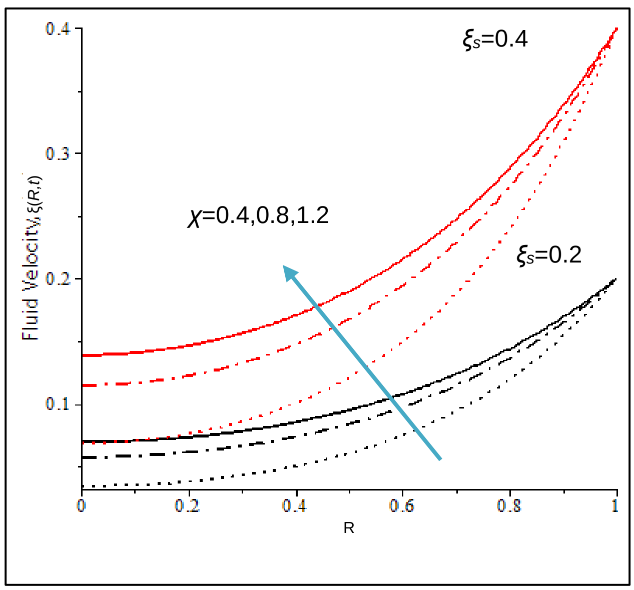

Figure 3. Effect of Casson Parameters on velocity distributions (α=0.3, Da=M=t=1)

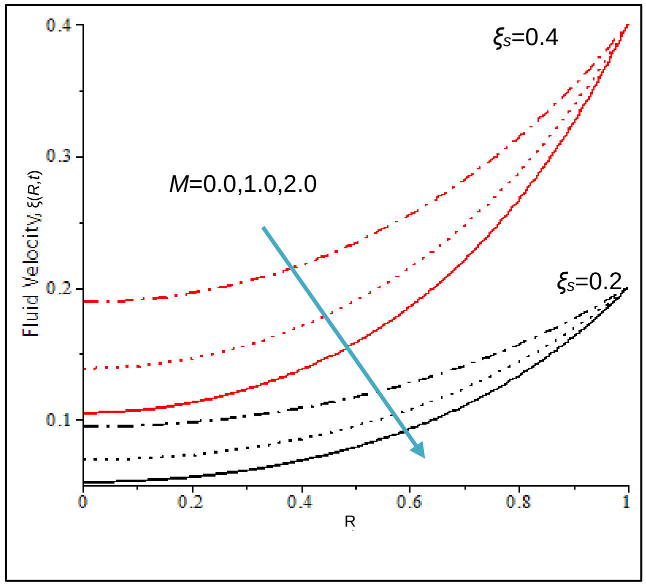

Figure 4. Effect of Magnetic Parameters on velocity distributions (α=0.3, χ=1.2, *Da*=*t*=1)

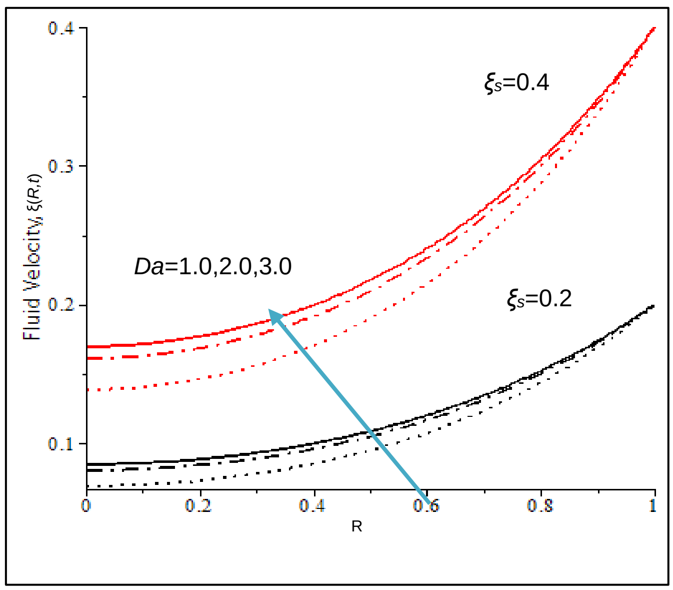

Figure 5. Effect of Darcy Numbers on velocity distributions (α=0.3, χ=1.2, *M*=*t*=1)

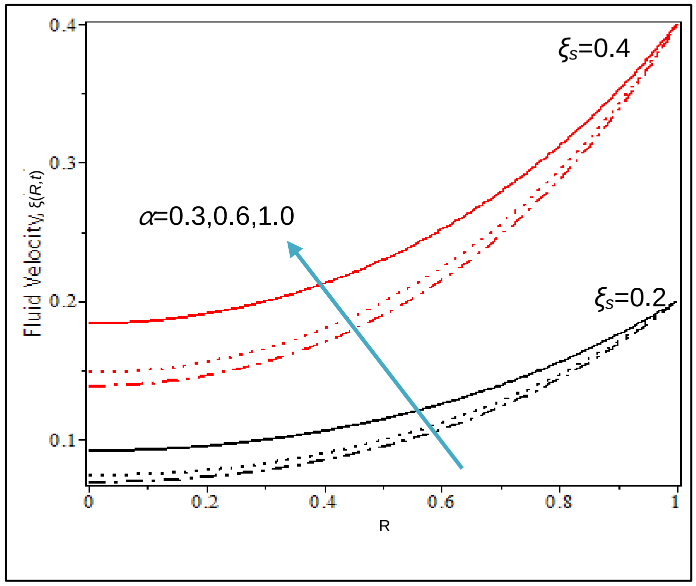

Figure 6. Effect of fractional parameter on velocity distributions (χ=1.2, *Da*=*M*=*t*=1)

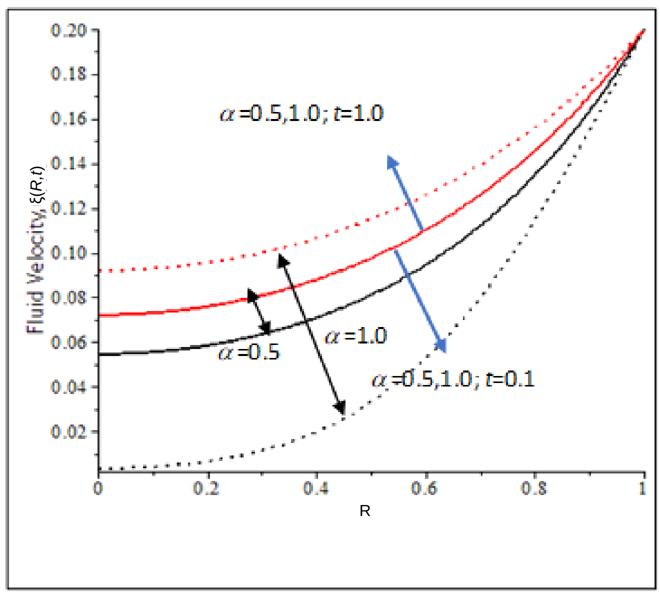

Figure 7. Effect of fractional and time parameters on velocity distributions (χ=1.2, ξ_s=0.2, *Da*=*M*=1)

Conclusions

In this investigation, the Caputo-Fabrizio fractional Casson fluid model is examined within a cylindrical context to evaluate the impact of MHD, porosity, and slip velocity on the system. Laplace and finite Hankel transform methods are employed to obtain analytical solutions, with particular attention to ensuring compliance with the necessary initial and boundary conditions. Below are the summarized outcomes:

i. The results align consistently with the established analytical solution's limiting case and previously reported findings, affirming the validity of our proposed solution.
ii. Higher values of χ, *Da*, α, ξ_s, and *t* lead to greater fluid velocity.
iii. Conversely, higher values of *M* correspond to lower fluid velocity.
iv. Elevated fractional parameters correspond to heightened fluid velocity over an extended period,

while lower values yield the opposite effect.

v. The fractional fluid model offers enhanced accuracy and realism in comparison to the classical fluid model.

vi. Fluid flow is significantly enhanced by slip velocity, especially at the cylinder wall (R=1).

This research holds particular significance in comprehending blood flow in small human arteries to provide early hypotheses for blood-disease treatment such as cancer, fatty plaque, and others. Furthermore, it functions as a valuable tool for validating the precision of numerical solutions.

Conflicts of Interest

The author(s) declare(s) that there is no conflict of interest regarding the publication of this paper.

Acknowledgment

The authors wish to express their gratitude for the financial assistance received from Universiti Teknologi Malaysia, which was provided through the Others Grant Scheme (R.J130000.7354.4B748) and the Matching Grant Scheme (Q.J130000.3054.03M77).

References

[1] N. J. Alderman and S. Pipelines. (1977). Non-Newtonian fluids: Guide to classification and characteristics. Technical Report.

[2] R. P. Chhabra. (2010). Non-Newtonian luids : An introduction. *SERC School-cum-Symposium on Rheology of Complex Fluids*, 1-33.

[3] R. L. Batra and B. Das. (1992). Flow of a Casson fluid between two rotating cylinders. *FLuid Dyn. Res.*, *9*, 133-141,

[4] J. R. Keltner, M. S. Roos, P. R. Brakeman, and T. F. Budinger. (1990). Magnetohydrodynamics of blood flow. *Magn. Reson. Med.*, *161*, 139-149.

[5] A. Sinha, J. C. Misra, and G. C. Shit. (2016). Effect of heat transfer on unsteady MHD flow of blood in a permeable vessel in the presence of non-uniform heat source. *Alexandria Eng. J.*, *55*(3), 2023-2033.

[6] V. K. Sud and G. S. Sekhon. (1989). Blood flow through the human arterial system in the presence of a steady magnetic field. *Phys. Med. Biol.*, *34*(7), 795-805.

[7] E. F. Elshehawey, E. M. E. Elbarbary, N. A. S. Afifi, and M. El-Shahed. (2001). MHD flow of blood under body acceleration. *Integr. Transform. Spec. Funct.*, *121*, 1-6.

[8] E. E. Tzirtzilakis. (2005). A mathematical model for blood flow in magnetic field. *Phys. Fluids*, *17*(7), 1-15.

[9] D. C. Sanyal, K. Das, and S. Debnath. (2007). Effect of magnetic field on pulsatile blood flow through an inclined circular tube with periodic body acceleration. *11*(December 2014), 43-56.

[10] R. K. Dash, K. N. Mehta, and G. Jayaraman. (1996). Casson fluid flow in a pipe filled with a Homogeneous porous medium. *Int. J. Engng Sci.*, *34*(10), 1145-1156.

[11] T. Sochi. (2010). Non-Newtonian flow in porous media. *Polymer (Guildf)*, *51*(22),5007-5023.

[12] E. F. Elshehawey, W. M. E. Elbarbary, N. A. S. Afifi, and M. El-Shahed. (2000). Pulsatile flow of blood through a stenosed porous medium under periodic body acceleration. *Int. J. Theor. Phys.*, *39*(1), 183-188.

[13] V. P. Rathod and S. Tanveer. (2009). Pulsatile flow of couple stress fluid through a porous medium with periodic body acceleration and magnetic field. *Bull. Malaysian Math. Sci. Soc.*, *32*(2), 245-259.

[14] M. Jamil and M. Zafarullah. (2019). MHD flows of second grade uid through the moving porous cylindrical domain. *Eur. J. Pure Appl. Math.*, *12*(3), 1149-1175.

[15] I. J. Rao and K. R. Rajagopal. (1999). Effect of the slip boundary condition on the flow of fluids in a channel. *Acta Mech.*, *135*(3), 113-126.

[16] Y. Nubar, “Blood Flow, Slip, and Viscometry. (1971). *Biophys. J.*, *11*, 252-264.

[17] M. A. Imran, S. Sarwar, and M. Imran. (2016). Effects of slip on free convection flow of Casson fluid over an oscillating vertical plate. *Bound. Value Probl.*, *2016*(1), 1-11.

[18] J. Nandal, S. Kumari, and R. Rathee. (2019). The Effect of slip velocity on unsteady peristalsis MHD blood flow through a constricted artery experiencing body acceleration. *Int. J. Appl. Mech. Eng.*, *24*(3), 645-659.

[19] K. Ramesh and M. Devakar. (2015). Some analytical solutions for flows of Casson fluid with slip boundary conditions. *Ain Shams Eng. J.*, *6*(3), 967-975.

[20] R. Padma, R. Ponalagusamy, and R. Tamil Selvi. (2019). Mathematical modeling of electro hydrodynamic non-Newtonian fluid flow through tapered arterial stenosis with periodic body acceleration and applied magnetic field. *Appl. Math. Comput.*, *362*, 124453.

[21] R. Padma, R. T. Selvi, and R. Ponalagusamy. (2019). Effects of slip and magnetic field on the pulsatile flow of a Jeffrey fluid with magnetic nanoparticles in a stenosed artery. *Eur. Phys. J. Plus*, *134*, 1-15.

[22] S. Ahmed and G. C. Hazarika. (2012). Casson fluid model for blood flow with velocity slip in presence of magnetic effect. *Int. J. Sci. Basic Appl. Res.*, *5*(1), 1-8.

[23] M. Jalil and W. Iqbal. (2021). Numerical analysis of suction and blowing effect on boundary layer slip flow of Casson fluid along with permeable exponentially stretching cylinder.*AIP Adv.*, *11*(3).

[24] A. Shaikh, A. Tassaddiq, K. S. Nisar, and D. Baleanu. (2019). Analysis of differential equations involving

Caputo–Fabrizio fractional operator and its applications to reaction–diffusion equations. *Adv. Differ. Equations*, *2019*(1).
[25] B. Ross. (1975). A brief history and exposition of the fundamental theory of fractional calculus. *Fract. Calc. its Appl.*, *57*, 1-36.
[26] V. V Kulish and J. L. Lage. (2002). Application of fractional calculus to fluid mechanics. *J. Fluids Eng.*, 124(September), 803-808.
[27] G. A. M. B. Nchama. (2020). Properties of caputo-fabrizio fractional operators. *New Trends Math. Sci.*, *1*(8), 001-025.
[28] D. Kumar and J. Singh. (2020). *Fractional calculus in medical and heakth science*. CRC Press.
[29] F. Ali, N. A. Sheikh, I. Khan, and M. Saqib. (2017). Magnetic field effect on blood flow of Casson fluid in axisymmetric cylindrical tube: A fractional model. *J. Magn. Magn. Mater.*, *423*(May 2016), 327-336.
[30] N. Sene. (2022). Analytical solutions of a class of fluids models with the caputo fractional derivative. *Fractal Fract.*, *6*(1).
[31] F. E. G. Bouzenna, M. T. Meftah, and M. Difallah. (2020). Application of the Caputo–Fabrizio derivative without singular kernel to fractional Schrödinger equations. *Pramana - J. Phys.*, *94*(1), 1-7.
[32] F. Ali, A. Imtiaz, I. Khan, and N. A. Sheikh. (2018). Flow of magnetic particles in blood with isothermal heating: A fractional model for two-phase flow. *J. Magn. Magn. Mater.*, *456*, 413-422.
[33] F. Ali, N. Khan, A. Imtiaz, I. Khan, and N. A. Sheikh. (2019). The impact of magnetohydrodynamics and heat transfer on the unsteady flow of Casson fluid in an oscillating cylinder via integral transform: A Caputo–Fabrizio fractional model. *Pramana - J. Phys.*, *93*(3), 1-12.
[34] F. Ali, A. Imtiaz, I. Khan, and N. A. Sheikh. (2018). Hemodynamic flow in a vertical cylinder with heat transfer: Two-phase caputo fabrizio fractional model, *J. Magn.*, *23*(2), 179-191.
[35] S. Maiti, S. Shaw, and G. C. Shit. (2020). Caputo–Fabrizio fractional order model on MHD blood flow with heat and mass transfer through a porous vessel in the presence of thermal radiation. *Phys. A Stat. Mech. its Appl.*, *540*, 123149.
[36] S. Maiti, S. Shaw, and G. C. Shit. (2021). Fractional order model for thermochemical flow of blood with Dufour and Soret effects under magnetic and vibration environment. *Colloids Surfaces B Biointerfaces*, *197*(October 2020), 111395.
[37] S. Maiti, S. Shaw, and G. C. Shit. (2021). Fractional order model of thermo-solutal and magnetic nanoparticles transport for drug delivery applications. *Colloids Surfaces B Biointerfaces*, *203*(March), 111754.
[38] S. Maiti, S. Shaw, and G. C. Shit. (2021). Fractional order model for thermochemical flow of blood with Dufour and Soret effects under magnetic and vibration environment. *Colloids Surfaces B Biointerfaces*, *197*(September 2020), 111395,
[39] D. F. Jamil, S. Uddin, M. G. Kamardan, and R. Roslan. (2020).The effects of magnetic blood flow in an inclined cylindrical tube using caputo-fabrizio fractional derivatives. *CFD Lett. J.*, 1(1), 111-122.
[40] D. F. Jamil, S. Uddin, and R. Roslan. (2020). The Effects of Magnetic Casson Blood Flow in an Inclined Multi-stenosed Artery by using Caputo-Fabrizio Fractional Derivatives. *J. Adv. Res. Mater. Sci.*, 1(1), 15-30.
[41] D. F. Jamil, S. Saleem, R. Roslan, M. Rahimi-gorji, A. Issakhov, and S. Ud Din. (2021). Analysis of non-Newtonian magnetic Casson blood flow in an inclined stenosed artery using Caputo-Fabrizio fractional derivatives. *Comput. Methods Programs Biomed.*, *203*, 106044.
[42] I. Khan, N. A. Shah, A. Tassaddiq, N. Mustapha, and S. A. Kechil. (2018). Natural convection heat transfer in an oscillating vertical cylinder. *PLoS One*, *13*(1), e0188656.